RESEARCH ARTICLE

Skeletal muscle-derived cells repair peripheral nerve defects in mice

Zi-Xiang Chen[1], Hai-Bin Lu[1], Xiao-Lei Jin[1], Wei-Feng Feng[2], Xiao-Nan Yang[1,*], Zuo-Liang Qi[1,*]
1 The 16th Department, Plastic Surgery Hospital, Chinese Academy of Medical Sciences (CAMS) and Peking Union Medical College (PUMC), Beijing, China
2 Yu Tian Cheng Plastic Surgery Clinic, Shanghai, China

Funding: *This study was financially supported by the National Natural Science Foundation of China, No. 81671908 (to ZLQ) and No. 81571921 (to XNY); the Fundamental Research Fund for the Central Universities of China, No. 2016ZX310197 (to ZLQ); the Union Youth Science & Research Foundation of China, No. 3332015155 (to XNY); the Science Fund of Plastic Surgery Hospital, Chinese Academy of Medical Sciences, and Peking Union Medical College of China, No. Q2015013 (to XNY).*

Graphical Abstract

Muscle-derived cells (MDCs) promote the regeneration of peripheral nerves, which is confirmed by morphological, histological and functional assessments

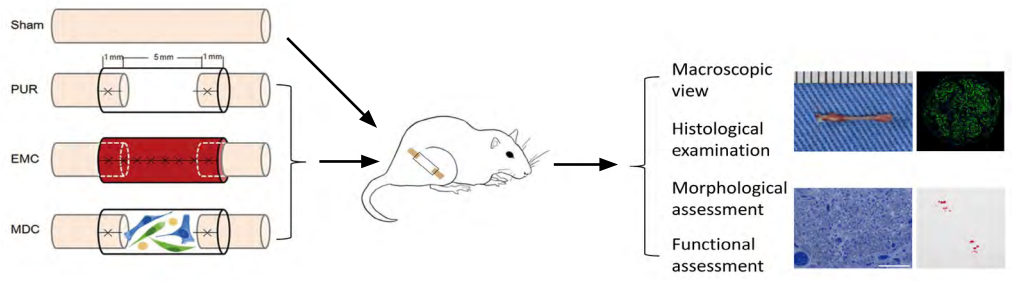

Correspondence to:
Xiao-Nan Yang, MD, PhD, yxnan@aliyun.com;
Zuo-Liang Qi, MD, PhD, public_qi@163.com.

orcid:
0000-0002-3335-7669 (Xiao-Nan Yang)
0000-0002-8730-065X (Zuo-Liang Qi)

doi: *10.4103/1673-5374.264462*

Received: *February 20, 2019*
Accepted: *July 15, 2019*

Abstract

Skeletal muscle-derived cells have strong secretory function, while skeletal muscle-derived stem cells, which are included in muscle-derived cells, can differentiate into Schwann cell-like cells and other cell types. However, the effect of muscle-derived cells on peripheral nerve defects has not been reported. In this study, 5-mm-long nerve defects were created in the right sciatic nerves of mice to construct a peripheral nerve defect model. Adult female C57BL/6 mice were randomly divided into four groups. For the muscle-derived cell group, muscle-derived cells were injected into the catheter after the cut nerve ends were bridged with a polyurethane catheter. For external oblique muscle-fabricated nerve conduit and polyurethane groups, an external oblique muscle-fabricated nerve conduit or polyurethane catheter was used to bridge the cut nerve ends, respectively. For the sham group, the sciatic nerves on the right side were separated but not excised. At 8 and 12 weeks post-surgery, distributions of axons and myelin sheaths were observed, and the nerve diameter was calculated using immunofluorescence staining. The number, diameter, and thickness of myelinated nerve fibers were detected by toluidine blue staining and transmission electron microscopy. Muscle fiber area ratios were calculated by Masson's trichrome staining of gastrocnemius muscle sections. Sciatic functional index was recorded using walking footprint analysis at 4, 8, and 12 weeks after operation. The results showed that, at 8 and 12 weeks after surgery, myelin sheaths and axons of regenerating nerves were evenly distributed in the muscle-derived cell group. The number, diameter, and myelin sheath thickness of myelinated nerve fibers, as well as gastrocnemius muscle wet weight and muscle area ratio, were significantly higher in the muscle-derived cell group compared with the polyurethane group. At 4, 8, and 12 weeks post-surgery, sciatic functional index was notably increased in the muscle-derived cell group compared with the polyurethane group. These criteria of the muscle-derived cell group were not significantly different from the external oblique muscle-fabricated nerve conduit group. Collectively, these data suggest that muscle-derived cells effectively accelerated peripheral nerve regeneration. This study was approved by the Animal Ethics Committee of Plastic Surgery Hospital, Chinese Academy of Medical Sciences (approval No. 040) on September 28, 2016.

Key Words: *muscle nerve conduit; myokine; nerve regeneration; nerve repair; peripheral nerve regeneration; polyurethane catheter; seed cells; skeletal muscle; skeletal muscle-derived cells; tissue-engineered nerve*

Chinese Library Classification No. *R459.9; R363; R364*

Introduction

The gold standard for treatment of peripheral nerve defects is nerve autografting. However, because of its limitations, such as a finite number of donated nerves and increased morbidity at donor sites (de Medinaceli et al., 1993; Kim et al., 2003), an alternative option with satisfactory outcomes for repairing peripheral nerve defects is still needed.

Seeding nerve conduits with cells is currently a promising technique for peripheral nerve tissue engineering. Seeded cells include Schwann cells, Schwann-like cells, skin-derived precursors, and different kinds of stem cells, e.g. embryonic stem cells, bone marrow-derived mesenchymal stem cells, and adipose-derived stem cells (Walsh et al., 2009; Fan et al., 2014; Jiang et al., 2016; Sowa et al., 2016; Xiang et al., 2017; Zheng et al., 2017; Cao et al., 2019), which can participate in peripheral nerve repair through their differentiation, secretion, or delivery functions (Pang et al., 2013; Fan et al., 2014; Jiang et al., 2016, 2017). Therefore, we suspected that cells with the potential to both secrete neurotrophic factors and differentiate into cellular components of peripheral nerves may be used as a source of seed cells to promote nerve repair.

Sections of skeletal muscle have been used to bridge peripheral nerve defects for a number of decades and have demonstrated promising results towards peripheral nerve recovery (Brunelli et al., 1993; Battiston et al., 2000; Geuna et al., 2004; Meek et al., 2004; Ronchi et al., 2018). Another effective method involves the fabrication of fresh mouse muscles into a hollow nerve conduit, termed an external oblique muscle-fabricated nerve conduit (EMC), to repair sciatic nerve defects (Yang et al., 2013). Thus, the cellular components of muscle may play an important role in the repair process.

Skeletal muscle-derived cells (MDCs) consist of myocytes, fibroblasts, muscle progenitor cells, and muscle-derived stem cells (MDSCs) (Chen et al., 2016; Weng et al., 2018). MDCs secrete up to 300 factors, known as myokines, such as brain-derived neurotrophic factor (Le Bihan et al., 2012; Raschke et al., 2013; Hartwig et al., 2014). In addition, MDSCs can differentiate into Schwann cell-like cells *in vivo* and *in vitro* (Lavasani et al., 2014; Tamaki et al., 2014). To our knowledge, however, MDCs have not been utilized as a cell source for peripheral nerve reconstruction. Thus, we speculated that MDCs could have therapeutic potential for peripheral nerve repair. This study aimed to assess the capability of MDCs to promote peripheral nerve regeneration.

Materials and Methods

Animals

Wide-type, female, 8-week-old C57BL/6 mice (n = 80), weighing 22–24 g, were obtained from Vital River Laboratory Animal Technology [Beijing, China; License No. SYXK (Jing) 2015-0009]. Mice, fed with normative murine food and water, were housed with 12-hour light/dark cycles. This study was approved by the Animal Ethics Committee of Plastic Surgery Hospital, Chinese Academy of Medical Sciences (approval No. 040) on September 28, 2016. All animal care and animal surgeries were performed in strict conformity with the National Institutes of Health (NIH) Guide for the Care and Use of Laboratory Animals (NIH Publication No. 85-23, revised 1985).

Prior to surgery, a total of 64 C57BL/6 mice were randomly and evenly assigned to four groups: sham (n = 16, nerves were exposed without excision), polyurethane (PUR; n = 16, cut nerve ends were bridged with a polyurethane catheter), EMC (n = 16, cut nerve ends were bridged with an EMC), and MDC (n = 16, cut nerve ends were bridged with a polyurethane catheter seeded with MDCs). Eight mice were sampled from each group at each time point; four were used for frozen sectioning and immunofluorescence staining, while the others were used for transmission electron microscopy (TEM; JOEL, Tokyo, Japan).

Cell culture and identification

MDCs were isolated from eight C57BL/6 mice and cultured according to a previously reported protocol (Chen et al., 2016). Mice were anesthetized by intraperitoneal injection using pentobarbital sodium (0.05 mg/g body weight; Sigma, Shanghai, China). Briefly, skeletal muscles of mouse hind limbs were explanted and cut into 1-mm^3 fragments, which were enzyme-digested with 2.4 U/mL dispase (Solarbio, Beijing, China) and 0.2% collagenase II (Sigma, Saint Louis, MO, USA) in Dulbecco's Modified Eagle's Medium (DMEM) (Hyclone, Logan City, UT, USA) at 37°C for 2 hours. After filtration with a sterile 70-μm cell strainer (Corning, NY, USA), cells were centrifuged and cultured with DMEM containing 10% fetal bovine serum (Gibco-AUS, Thornton, NSW, Australia). The density of seeded cells was 2×10^4 cells per 1 cm^2. The medium was replaced every 72 hours. Cells were subcultured at the same density when confluency exceeded 80%. Passage 1 MDCs were applied for all subsequent procedures.

After fixation of cultured cells with 4% paraformaldehyde, MDCs were washed, followed by a rinse with 0.1% Triton X-100. After blocking, cell phenotypes were assessed by staining with rabbit anti-vimentin (1:250; Abcam, Cambridge, UK), mouse anti-MyoD (1:100; Abcam), and rabbit anti-desmin (1:100; Abcam) antibodies at 4°C for at least 8 hours. MDCs were then incubated with Alexa Fluor 594-conjugated goat anti-rabbit (Abcam) or Alexa Fluor 488-conjugated goat anti-mouse (Abcam) IgG secondary antibodies. Nuclei of MDCs were stained with 4′,6-diamidino-2-phenylindole (DAPI; Solarbio). Stained cells were observed by fluorescent microscopy (Leica, Wetzlar, Germany) and images were obtained.

Fabrication of skeletal muscle nerve conduits

Eight C57BL/6 mice were used for the preparation of skeletal muscle nerve conduits (Yang et al., 2013). Mice were anesthetized by intraperitoneal injection using pentobarbital sodium (0.05 mg/g weight; Sigma). An incision on the lower dorsal part was created after shaving and sterilizing. Subcutaneous layers were separated to expose the external oblique muscle (**Figure 1A**), which was then explanted. The inner

side was carefully trimmed to expose the muscle fibers and cut into a 7 mm-long thin slice (**Figure 1B**). This inner side was folded inwards and wrapped around a 25-gauge syringe needle, while the two long lateral edges of the thin slice were discontinuously stitched with 11-0 sutures to form an EMC (**Figure 1C** and **D**).

Surgical procedures

Surgery was performed on the right hind limb. After anesthesia induction with pentobarbital sodium, the retral skin of the operated limb was incised. The sciatic nerve was exposed after the separation of skin and gluteal musculature. Sciatic nerves on the right side of sham group mice were separated but not excised (Sowa et al., 2016). For EMC and PUR groups, the 5-mm long sciatic nerve was removed, and a 5-mm gap between was created between the cut ends. The two nerve stumps were bridged with an EMC or PUR conduit (both 7-mm long), and stitched with 11-0 sutures to guarantee a 5-mm long defect left between the cut ends (Yang et al., 2013). A 2 μL mixture of DMEM and Matrigel (BD Biocoat, Bedford, MA, USA) in equal parts was injected into the EMC or PUR conduit. For the MDC group, after bridging the two cut ends with the PUR conduit and leaving a 5-mm gap, 2×10^4 MDCs in a 2 μL mixture of DMEM and Matrigel in equal parts was slowly injected inside. The skin incision was closed. Animals were allowed to recuperate with access to food and water.

At 8 and 12 weeks post-surgery, mice were sampled after anesthesia was induced by intraperitoneal injection with pentobarbital sodium (0.05 mg/g weight; Sigma). Both the nerve segment and gastrocnemius muscle on the repaired side were harvested for further examination. In each group, nerve samples were collected from eight mice at each time point, four of which were used for frozen sectioning, while the others were prepared for TEM.

Histological examination

At 8 and 12 weeks post-surgery, a 3-mm segment from the middle of the nerve was harvested from the repaired site. After fixation with 4% paraformaldehyde for 24 hours and dehydration with sucrose solution (20%) at 4°C for 24–48 hours, nerve samples were embedded with Optimal Cutting Temperature compound, and sliced into 8 μm-thick frozen transverse sections. Sections were then rinsed with phosphate-buffered saline (PBS), 0.3% Triton X-100, and blocked with 10% normal goat serum. Nerve sections were subsequently incubated with rabbit anti-neurofilament heavy (NF-H) polypeptide (1:500; Abcam) or rabbit anti-S100β (1:200; Abcam) antibody overnight at 4°C. After washing, sections were incubated with Alexa Fluor 488- or Alexa Fluor 594-conjugated goat anti-rabbit IgG (Abcam) secondary antibodies. Cell nuclei were counterstained with DAPI. Slides were viewed and imaged using fluorescent microscopy (Leica). Nerve diameters were measured from immunofluorescence staining images of nerve cross-sections using ImageJ v1.51 software (NIH, Bethesda, MD, USA). Four images from each group were measured.

Morphological assessment

Eight and 12 weeks after operation, sampled nerve specimens were immersed in 2.5% glutaraldehyde at 4°C overnight for fixation. The following day, samples were rinsed in PBS, fixed with 1% osmic acid, then dehydrated in a serial gradient of ethanol. Samples were then immersed in epoxy resin with acetone and embedded in epoxy resin 812 (Zhongxingbairui, Beijing, China). Segmented nerves were subsequently cut into 1-μm semi-thin sections and mounted on slides, which were dyed with 1% toluidine blue and imaged (Leica). Images of toluidine blue-staining at 200× were used to count numbers of myelinated nerve fibers. In addition, embedded samples were sliced into 50-nm ultrathin sections, stained with lead citrate, and observed by TEM. Circumferences of axonal and myelinated nerve fibers were scaled from 6000× images using ImageJ v1.51 software. At least 100 nerve fibers in each group were measured. From these dimensions, myelin sheath thickness and the diameter of each myelinated nerve fiber were calculated using ImageJ v1.51 software.

Walking footprint analysis

Four, 8, and 12 weeks post-operation, walking track assessments of all animals that had not been sacrificed at each time point were performed. Briefly, the hind paws of these mice were dipped in red ink and they were permitted to walk on the surface of white paper. Sciatic functional index (SFI) was counted for each footprint. At least 5 footprints from each group were evaluated using the equation: $SFI = -51.2 \times [(EPL - NPL)/NPL] + 118.9 \times [(ETS - NTS)/NTS] - 7.5$, where EPL is the experimental print length, NPL is the normal print length, ETS is experimental toe spread, and NTS is normal toe spread (Inserra et al., 1998).

Gastrocnemius muscle wet weight and Masson's trichrome staining

Eight and 12 weeks post-surgery, the gastrocnemius muscle from each repaired side was harvested, blotted with absorbent paper, and evaluated for wet weight. Next, muscles were fixed in 4% paraformaldehyde, dehydrated with a serial gradient of ethanol, and cleared in xylene. Afterwards, specimens were embedded in paraffin and sectioned into 5-μm slices, which were dyed with Masson's trichrome (Solibor, Beijing, China) and observed under a microscope (Leica). Digital images were captured and ratios of muscle fiber area to the total area were calculated using ImageJ v1.51 software.

Statistical analysis

All measurement data are represented as mean ± SD. Analyses were performed with GraphPad Prism 6.0 software (La Jolla, CA, USA). Diameters of myelinated nerve fibers, thicknesses of myelin sheaths, and SFI values were compared between groups at each time point using one-way analysis of variance followed by Bonferroni *post hoc* test. Other data were compared between groups at the same time point using one-way analysis of variance followed by Tukey's *post hoc* test. A value of $P < 0.05$ was considered statistically significant.

Results

Characterization of MDCs

Immunofluorescence staining demonstrated that MDCs expressed fibroblast (vimentin) (**Figure 2A** and **B**) and myogenic cell (MyoD and desmin) biomarkers (**Figure 2C–F**), confirming that MDCs are a mixed cell population exhibiting multiple morphologies. These results were consistent with a previous study (Chen et al., 2012).

Diameter and distribution of regenerating myelinated nerves are restored by MDCs

All mice survived without complications. Macroscopic views of regenerating nerves of mice in the four groups at 12 weeks post-operation are presented in **Figure 3**. Regenerated nerves from the PUR group (**Figure 3B**) were slimmer than observed in EMC (**Figure 3C**) and MDC (**Figure 3D**) groups. The muscle-fabricated conduit of the EMC group was well preserved. The appearance of regenerated nerves in the MDC group was intact.

Figure 4 shows NF-H and S100β immunofluorescence staining of regenerating nerves at 8 and 12 weeks post-surgery. In the sham group (**Figure 4A**, **E**, **I**, and **M**), NF-H-expressing axons (represented by a pitting form) and S100β-expressing myelin sheaths (ring shapes) were evenly distributed. For the PUR group (**Figure 4B**, **F**, **J**, and **N**), the distribution of NF-H-expressing axons and S100β-expressing myelin sheaths were uniform but with a small scope. In the EMC group, most NF-H-positive axons were distributed along the wall of the conduit (**Figure 4C**), while S100β-positive myelin sheaths were not evenly distributed at 8 weeks post-surgery (**Figure 4G**). A portion of NF-H-expressing axons without the pitting form and S100β-positive myelin sheaths without ring shapes were observed, indicating that their arrangement was not parallel with the EMC. The distribution and shape of axons and myelin sheaths from the EMC group at 12 weeks post-surgery were improved (**Figure 4K**, and **O**). In the MDC group (**Figure 4D**, **H**, **L**, and **P**), NF-H-expressing axons and S100β-expressing myelin sheaths were uniformly distributed at both time points.

Diameters of nerves were measured from cross-sections of nerves (**Figure 5**). At 8 and 12 weeks post-surgery, the diameters of nerves in EMC and MDC groups were significantly increased compared with the PUR group ($P < 0.001$). Moreover, nerve diameters were larger in the EMC group compared with the MDC group ($P < 0.001$).

MDCs increase the number, diameter, and myelin sheath thickness of myelinated nerve fibers of regenerating nerves

To further investigate the amount of regeneration, numbers of regenerated myelinated nerve fibers in nerve segment groups were counted (**Figure 6A–H**). At 8 and 12 weeks post-surgery, myelinated nerve fibers from the sham group were uniformly distributed (**Figure 5E** and **6A**), unlike the other groups. At both 8 and 12 weeks post-surgery, myelinated nerve fiber numbers were notably higher in EMC and MDC groups compared with the PUR group ($P < 0.001$; **Figure 6I**). The difference in numbers of myelinated nerve fibers was significant between MDC and EMC groups ($P < 0.05$).

Ultrathin sections of nerve specimens are shown in **Figure 7**. At 8 and 12 weeks post-surgery, diameters of myelinated nerve fibers in the MDC group were significantly larger than in PUR and EMC groups; the difference in myelinated nerve fiber diameters between EMC and PUR groups was also significant. At 8 and 12 weeks post-surgery, myelin sheath thickness was significantly thicker in both EMC and MDC groups compared with the PUR group. Myelin sheath thickness was similar between MDC and EMC groups at 8 weeks post-surgery, but was thicker in the MDC group compared with the EMC group at 12 weeks post-surgery ($P < 0.01$).

MDC transplantation promotes motor function of sciatic nerve after impair

The motor function of mice was assessed using walking-track analysis (**Figure 8A–D**), with the results expressed as SFI. Twelve weeks post-surgery, experimental toe spreads of MDC (**Figure 8D**) and EMC (**Figure 8C**) groups were larger than observed in the PUR group (**Figure 8B**). SFI was notably higher in MDC and EMC groups compared with the PUR group at 4, 8, and 12 weeks post-surgery (**Figure 8E**). SFI was higher in the MDC group than in the EMC group at 8 weeks post-surgery ($P < 0.001$).

MDCs improves gastrocnemius muscle recovery from atrophy

Recovery of the gastrocnemius muscle from atrophy was assessed by the wet weight of gastrocnemius muscles. Recovery was also evaluated by calculating muscle area ratios of sections with Masson's trichrome staining. Depending on the macroscopic appearance of gastrocnemius muscles (**Figure 9A–D**) and Masson's trichrome-stained sections (**Figure 9E–H**) of repaired sites 12 weeks post-surgery, different extents of atrophy existed in the three repaired groups. Eight and 12 weeks post-surgery, gastrocnemius muscle wet weights were notably increased in MDC and EMC groups compared with the PUR group (**Figure 9I**). The MDC group exhibited increased muscle weight at 8 weeks post-surgery ($P < 0.001$), but was not statistically different at 12 weeks compared with the EMC group.

Sections with Masson's trichrome staining showed that different degrees of collagen deposition existed in gastrocnemius muscle fibers of the three repaired groups (**Figure 9F–H**). Ratios of muscle area were larger at 8 weeks post-surgery in the MDC group compared with EMC and PUR groups (**Figure 9J**). At 12 weeks post-surgery, muscle area ratios in MDC and EMC groups were both larger than observed in the PUR group. However, no significant difference was detected between EMC and MDC groups.

Discussion

Cell transplantation is a promising method to promote peripheral nerve regeneration. MDCs, with their powerful secretory function (Pedersen, 2011; Le Bihan et al., 2012; Raschke et al., 2013; Hartwig et al., 2014), are easily extracted

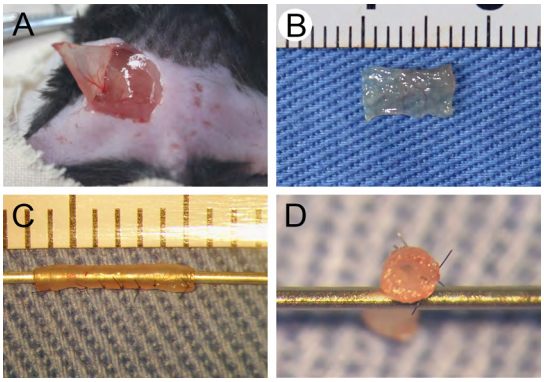

Figure 1 Fabrication of external oblique muscle-fabricated nerve conduit.
(A) An incision was made on the dorsal region close to the tail to expose the external oblique muscle. (B) The external oblique muscle was harvested, trimmed, and cut into a 7 mm-long thin slice. (C, D) The thin skeletal muscle tissue was discontinuously sutured into a hollow conduit.

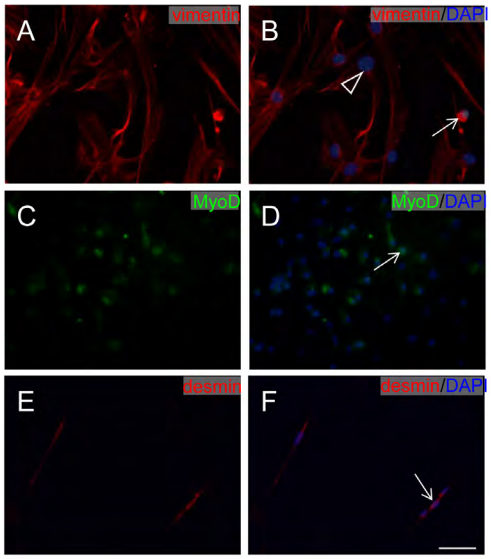

Figure 2 Immunofluorescence staining of muscle-derived cell markers.
(A, B) MDCs stained with vimentin (red). (C, D) MDCs stained with MyoD (green). (E, F) MDCs stained with desmin (red). All nuclei of cells were stained with 4′,6-diamidino-2-phenylindole (DAPI; blue). Scale bar: 100 μm. White arrows: muscle cells; white triangle: fibroblast. MDCs: Muscle-derived cells.

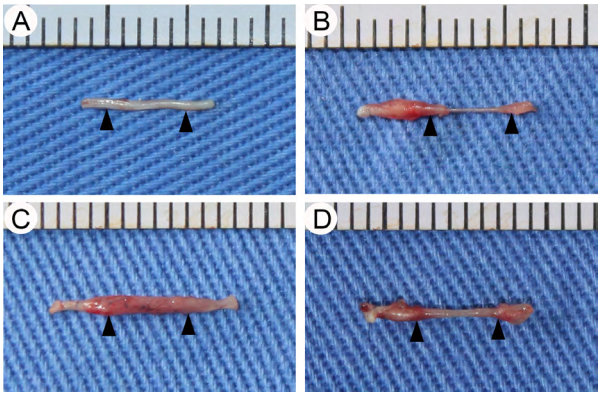

Figure 3 General observation of regenerating nerve at 12 weeks post-surgery.
(A–D) Regenerating nerves of sham, PUR, EMC, and MDC groups, respectively. Triangles indicate sites between the cut ends of the sciatic nerve filled by the regenerated nerve. EMC: External oblique muscle-fabricated nerve conduit; MDC: muscle-derived cell; PUR: polyurethane; Sham: sham-operated.

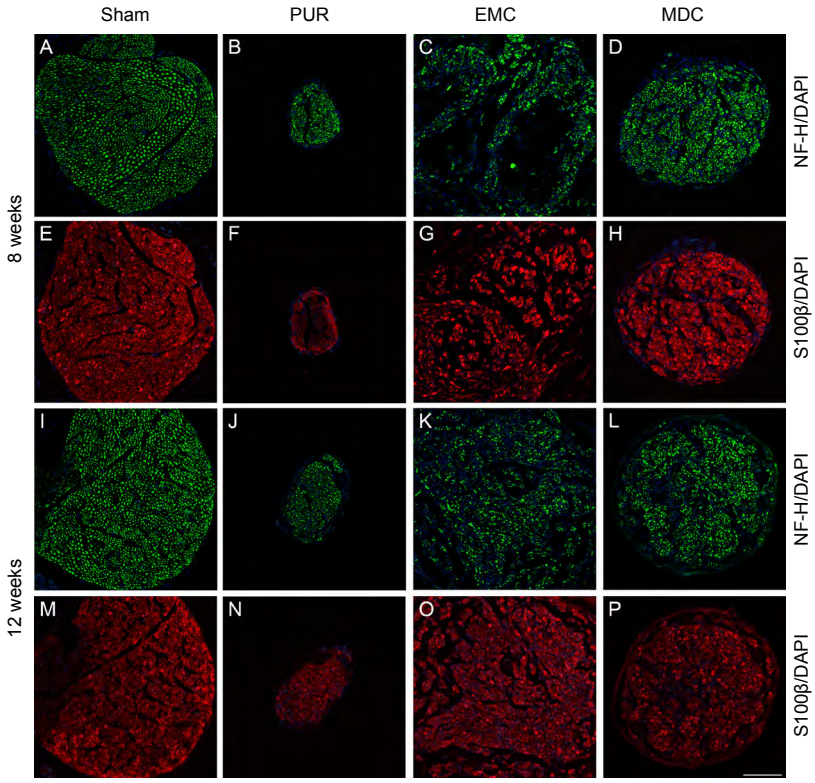

Figure 4 Immunofluorescence staining and distribution of nerve lesions at 8 and 12 weeks post-surgery.
(A–H) Eight weeks post-surgery; (I–P) twelve weeks post-surgery. (A, E, I, M) Sham group: NF-H-expressing axons and S100β-expressing myelin sheaths were evenly distributed. (B, F, J, N) PUR group: distributions of NF-H-expressing axons and S100β-expressing myelin sheaths were uniform but with a small scope. (C, G, K, O) EMC group: distributions of NF-H-positive axons and S100β-positive myelin sheaths were not uniform at 8 weeks post-surgery (C, G), but were improved at 12 weeks post-surgery (K, O). (D, H, L, P) MDC group: NF-H-expressing axons and S100β-expressing myelin sheaths were uniformly distributed at both time points. (A–D, I–L) NF-H (green); (E–H, M–P) S100β (red); 4′,6-diamidino-2-phenylindole (DAPI; blue). Scale bar: 100 μm. DAPI: 4′,6-Diamidino-2-phenylindole; EMC: external oblique muscle-fabricated nerve conduit; MDC: muscle-derived cell; NF-H: neurofilament heavy; PUR: polyurethane; Sham: sham-operated.

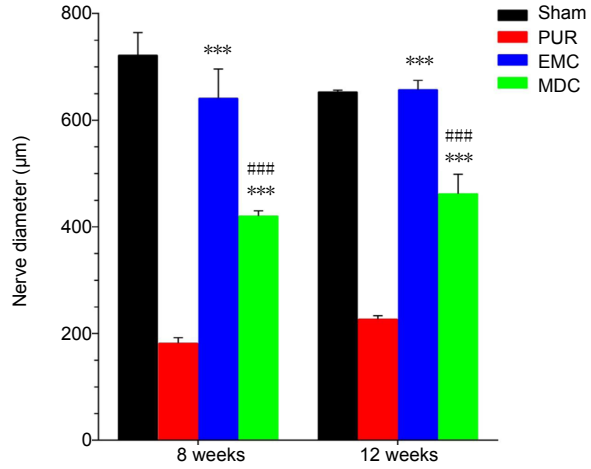

Figure 5 Statistical analysis of nerve diameters from cross-sections of the four groups at 8 and 12 weeks post-surgery.
At 8 and 12 weeks post-surgery, the diameters of nerves were larger in EMC and MDC groups compared with the PUR group. The EMC group had a larger nerve diameter compared with the MDC group. ***$P < 0.001$, *vs.* PUR group; ###$P < 0.001$, *vs.* EMC group. Data are expressed as the mean ± SD ($n = 4$; one-way analysis of variance followed by Tukey's *post hoc* test). EMC: External oblique muscle-fabricated nerve conduit; MDC: muscle-derived cell; PUR: polyurethane; Sham: sham-operated.

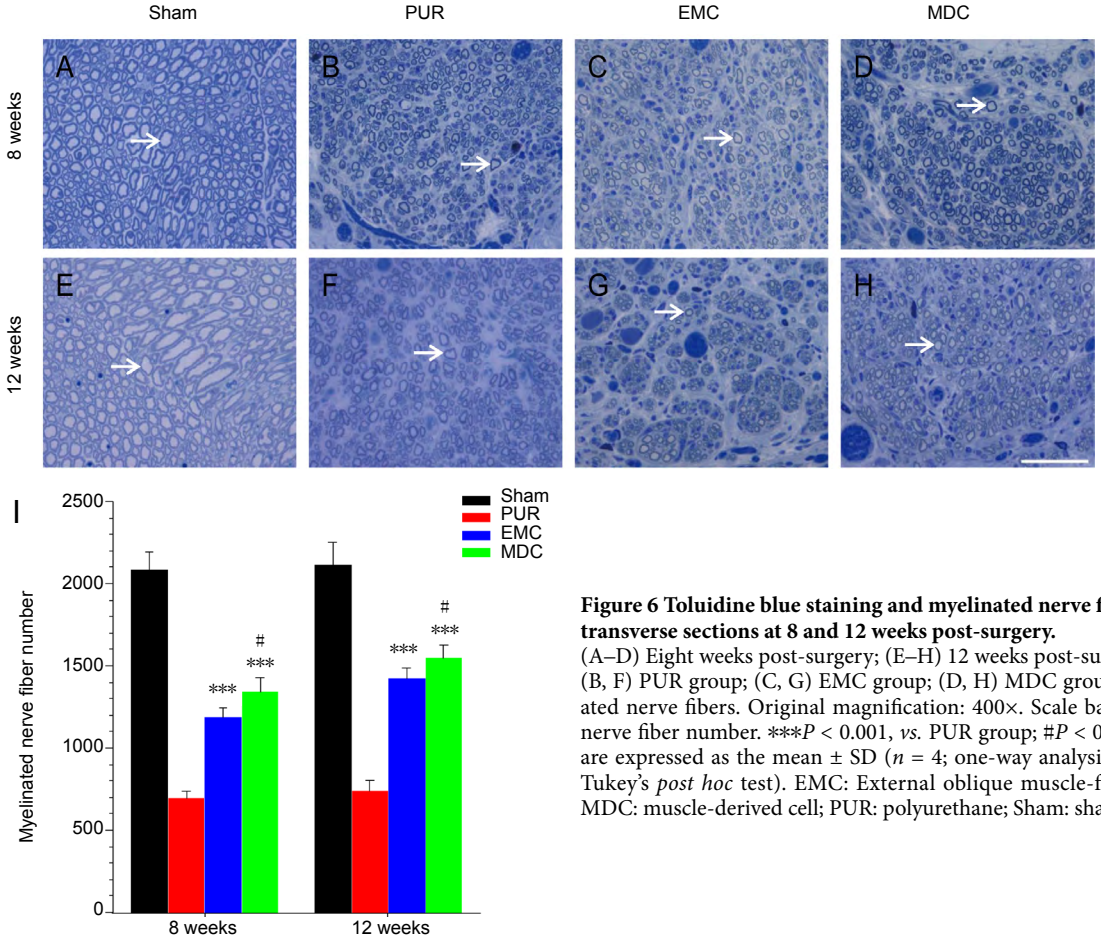

Figure 6 Toluidine blue staining and myelinated nerve fiber numbers of transverse sections at 8 and 12 weeks post-surgery.
(A–D) Eight weeks post-surgery; (E–H) 12 weeks post-surgery. (A, E) Sham group; (B, F) PUR group; (C, G) EMC group; (D, H) MDC group. White arrows: myelinated nerve fibers. Original magnification: 400×. Scale bar: 50 μm. (I) Myelinated nerve fiber number. ***$P < 0.001$, *vs.* PUR group; #$P < 0.05$, *vs.* EMC group. Data are expressed as the mean ± SD ($n = 4$; one-way analysis of variance followed by Tukey's *post hoc* test). EMC: External oblique muscle-fabricated nerve conduit; MDC: muscle-derived cell; PUR: polyurethane; Sham: sham-operated.

and cultured. Meanwhile, the MDSC component of MDCs, which can differentiate into mesoderm cells and ectoderm cells (Tamaki et al., 2007; Tamaki et al., 2014), can highly express antioxidants and survive under oxidative and hypoxic stresses (Urish et al., 2009; Vella et al., 2011). This study provides the first report of the effects of seeding nerve conduits with MDCs on repair of transected nerves. The results showed that compared with conduits alone, MDCs effectively (1) increased the diameter of the regenerated nerve; (2) increased the number and myelin sheath thickness of myelinated nerve fibers of the regenerated nerve; (3) promoted the recovery of motor function; and (4) increased the wet weight and reduced collagen deposition of gastrocnemius muscles. In addition, both MDC and EMC groups were noticeably superior to the PUR conduit alone for all measured criteria. These data indicate that MDCs effectively promoted peripheral nerve regeneration and could be a cell source for treating peripheral nerve diseases.

Previous studies have demonstrated the effectiveness of transplanting cells, such as Schwann cells and various types of stem cells, for repair of peripheral nerve defects (Fan et al., 2014; Jiang et al., 2016; Jiang et al., 2017). These cells promote peripheral nerve regeneration by secreting growth factors that accelerate Schwann cell migration or proliferation, differentiating into Schwann cell-like cells or neurons that participate in the construction of peripheral nerve tissue, or acting as transmitters of proximal and distal nerve messages (Pang et al., 2013; Fan et al., 2014; Jiang et al., 2016, 2017).

Immunofluorescence staining showed that the diameter of regenerating nerves was larger in MDC and EMC groups compared with the PUR group. Toluidine blue staining revealed increased numbers of myelinated nerve fibers in MDC and EMC groups compared with the PUR group. MDCs and fresh skeletal muscle both contain MDSCs, which have been shown to differentiate into Schwann cell-like cells *in vivo* and *in vitro*, and form myelin sheaths that participate in peripheral nerve reconstruction (Lavasani et al., 2014; Tamaki et al., 2014). In addition, MDSCs can differentiate into perineurial/endoneurial cells to form perineurium/endoneurium, which encircles regenerated axons (Tamaki et al., 2014). Otherwise, axons were wrapped with a skeletal muscle component when EMC was used to bridge nerve gaps in mice (Yang et al., 2013). These results indicate that MDSCs from MDCs and EMC participated in the construction of peripheral nerve tissue to promote peripheral nerve regeneration.

Immunofluorescence staining of sections indicated that myelin sheaths and axons of nerves from the MDC group were more evenly distributed compared with the EMC group at 8 weeks post-surgery. Further, the number and diameter of myelinated nerve fibers, SFI, muscle wet weight, and muscle area ratio indicated better outcomes in the MDC group at this time point compared with the EMC group. These phenomena suggest that the distribution of axons and myelin sheath in the peripheral nerve is strongly associated with functional recovery, as is the distribution of cells within nerve conduits. MDCs were uniformly distributed when seeded into PUR conduits in the MDC group. Hence, the up to 300 myokines secreted by MDCs (Pedersen, 2011; Le Bihan et al., 2012; Raschke et al., 2013; Hartwig et al., 2014) were likely evenly distributed within the catheter in the MDC group, while the concentration of myokines was relatively high close to the wall of the EMC. These myokines can induce Schwann cells, which provide a structural and bioactive environment that regulates both axonal regeneration after peripheral nerve impair (Brosius Lutz and Barres, 2014; Jessen and Mirsky, 2016; Gomez-Sanchez and Pilch, 2017) and nerve fiber growth towards them. Thus, nerve fibers of the EMC group at 8 weeks post-surgery were relatively concentrated close to the wall of the EMC, similar to the results of a previous study (Yang et al., 2013). These results suggest that the secretary function of MDCs could be another potential mechanism by which they participate in peripheral nerve repair.

Fresh skeletal muscles or EMC fabricated from fresh skeletal muscle have been shown to effectively promote peripheral nerve regeneration (Geuna et al., 2003, 2004; Yang et al., 2013). The effectiveness of MDCs for facilitating peripheral nerve repair was comparable with or even superior to that of EMC for criteria measured in the current study. Indeed, cells within the EMC required a longer time and distance to participate directly or indirectly in nerve reconstruction by migration along the nerve conduit. Moreover, with more EMC components, the effect of peripheral nerve repair may be more complicated.

Although our data indicated positive effects of MDCs on peripheral nerve regeneration, the underlying mechanisms are still unclear. MDCs are a mixed cell population for which, to our knowledge, there is still no uniform biomarker. Therefore, it is difficult to determine which cells in MDCs play a decisive role. Moreover, nerve repair is a complex procedure involving various cells and factors. Further experiments *in vitro* and *in vivo* are required to confirm the outcome of MDCs during peripheral nerve regeneration and verify the effects of MDCs on Schwann cells or neurons of peripheral nerves.

In summary, morphological, histological, and functional assessments confirmed that MDCs could accelerate the regeneration of peripheral nerves; indeed, observations were comparable to that of EMC. These data suggest that MDCs are an alternative and promising cell source for cell therapies targeting peripheral nervous system disorders and reconstruction of peripheral nerve defects. As such, the mechanism by which MDCs affect peripheral nerve repair is worthy of further studies.

Acknowledgments: *The authors thank Dr. Shuyi Wei from Minzu Hospital of Guangxi Zhuang Autonomous Region for helping sketch design.*
Author contributions: *Study design: ZXC, HBL, XNY, ZLQ; experimental studies: ZXC, HBL, WFF; data analysis: ZXC, XLJ, WFF, XNY; manuscript writing and editing: ZXC, XLJ, XNY, ZLQ. All authors reviewed and approved the manuscript.*
Conflicts of interest: *The authors declare that there are no conflicts of interest associated with this manuscript.*
Financial support: *This work was financially supported by the National Natural Science Foundation of China, No. 81671908 (to ZLQ) and No. 81571921 (to XNY); the Fundamental Research Fund for the Central Universities of China, No. 2016ZX310197 (to ZLQ); the Union Youth Science & Research Foundation of China, No. 3332015155 (to XNY); the Science Fund of Plastic Surgery Hospital, Chinese Academy of Medical Sciences, and Peking Union Medical College of China, No. Q2015013 (to XNY). The funding sources had no role in study conception and design, data analysis or interpretation, paper writing or deciding to submit this paper for publication.*
Institutional review board statement: *All experimental procedures and protocols were approved by the Experimental Animal Ethics Committee of Plastic Surgery Hospital, Chinese Academy of Medical Sciences University of China (approval No. 040) on September 28, 2016.*
Copyright license agreement: *The Copyright License Agreement has been signed by all authors before publication.*
Data sharing statement: *Datasets analyzed during the current study are available from the corresponding author on reasonable request.*
Plagiarism check: *Checked twice by iThenticate.*
Peer review: *Externally peer reviewed.*

identical terms.
Open peer reviewer: *Tufan Mert, University of Cukurova, Turkey.*
Additional file: *Open peer review report 1.*

References

Battiston B, Tos P, Geuna S, Giacobini-Robecchi MG, Guglielmone R (2000) Nerve repair by means of vein filled with muscle grafts. II. Morphological analysis of regeneration. Microsurgery 20:37-41.

Brosius Lutz A, Barres BA (2014) Contrasting the glial response to axon injury in the central and peripheral nervous systems. Dev Cell 28:7-17.

Brunelli GA, Battiston B, Vigasio A, Brunelli G, Marocolo D (1993) Bridging nerve defects with combined skeletal muscle and vein conduits. Microsurgery 14:247-251.

Cao P, Wang HN, Tian WF, Sun NC, Bai JB, Yu KL, Tian DH (2019) Human amniotic membrane repairs acute sciatic nerve injury in rat models. Zhongguo Zuzhi Gongcheng Yanjiu 23:1046-1051.

Chen B, Wang B, Zhang WJ, Zhou G, Cao Y, Liu W (2012) In vivo tendon engineering with skeletal muscle derived cells in a mouse model. Biomaterials 33:6086-6097.

Chen B, Ding J, Zhang W, Zhou g, Cao Y, Liu W, Wang B (2016) tissue engineering of tendons: a comparison of muscle-derived cells, tenocytes, and dermal fibroblasts as cell sources. Plast Reconstr Surg 137:536e-544e.

de Medinaceli L, Prayon M, Merle M (1993) Percentage of nerve injuries in which primary repair can be achieved by end-to-end approximation: review of 2,181 nerve lesions. Microsurgery 14:244-246.

Fan L, Yu Z, Li J, Dang X, Wang K (2014) Schwann-like cells seeded in acellular nerve grafts improve nerve regeneration. BMC Musculoskelet Disord 15:165.

Geuna S, Tos P, Battiston B, Giacobini-Robecchi MG (2004) Bridging peripheral nerve defects with muscle-vein combined guides. Neurol Res 26:139-144.

Geuna S, Raimondo S, Nicolino S, Boux E, Fornaro M, Tos P, Battiston B, Perroteau I (2003) Schwann-cell proliferation in muscle-vein combined conduits for bridging rat sciatic nerve defects. J Reconstr Microsurg 19:119-124.

Gomez-Sanchez JA, Pilch KS (2017) After nerve injury, lineage tracing shows that myelin and remak schwann cells elongate extensively and branch to form repair Schwann cells, which shorten radically on remyelination. J Neurosci 37:9086-9099.

Hartwig S, Raschke S, Knebel B, Scheler M, Irmler M, Passlack W, Muller S, Hanisch FG, Franz T, Li X, Dicken HD, Eckardt K, Beckers J, de Angelis MH, Weigert C, Häring HU, Al-Hasani H, Ouwens DM, Eckel J, Kotzka J, Lehr S (2014) Secretome profiling of primary human skeletal muscle cells. Biochim Biophys Acta 1844:1011-1017.

Inserra MM, Bloch DA, Terris DJ (1998) Functional indices for sciatic, peroneal, and posterior tibial nerve lesions in the mouse. Microsurgery 18:119-124.

Jessen KR, Mirsky R (2016) The repair Schwann cell and its function in regenerating nerves. J Physiol 594:3521-3531.

Jiang CQ, Hu J, Xiang JP, Zhu JK, Liu XL, Luo P (2016) Tissue-engineered rhesus monkey nerve grafts for the repair of long ulnar nerve defects: similar outcomes to autologous nerve grafts. Neural Regen Res 11:1845-1850.

Jiang L, Jones S, Jia X (2017) Stem cell transplantation for peripheral nerve regeneration: current options and opportunities. Int J Mol Sci 18:94.

Kim DH, Han K, Tiel RL, Murovic JA, Kline DG (2003) Surgical outcomes of 654 ulnar nerve lesions. J Neurosurg 98:993-1004.

Lavasani M, Thompson SD, Pollett JB, Usas A, Lu A, Stolz DB, Clark KA, Sun B, Peault B, Huard J (2014) Human muscle-derived stem/progenitor cells promote functional murine peripheral nerve regeneration. J Clin Invest 124:1745-1756.

Le Bihan MC, Bigot A, Jensen SS, Dennis JL, Rogowska-Wrzesinska A, Laine J, Gache V, Furling D, Jensen ON, Voit T, Mouly V, Coulton GR, Butler-Browne G (2012) In-depth analysis of the secretome identifies three major independent secretory pathways in differentiating human myoblasts. J Proteomics 77:344-356.

Meek MF, Varejao AS, Geuna S (2004) Use of skeletal muscle tissue in peripheral nerve repair: review of the literature. Tissue Eng 10:1027-1036.

Pang CJ, Tong L, Ji LL, Wang ZY, Zhang X, Gao H, Jia H, Zhang LX, Tong XJ (2013) Synergistic effects of ultrashort wave and bone marrow stromal cells on nerve regeneration with acellular nerve allografts. Synapse 67:637-647.

Pedersen BK (2011) Muscles and their myokines. J Exp Biol 214:337-346.

Raschke S, Eckardt K, Bjorklund Holven K, Jensen J, Eckel J (2013) Identification and validation of novel contraction-regulated myokines released from primary human skeletal muscle cells. PLoS One 8:e62008.

Ronchi G, Fornasari BE, Crosio A, Budau CA, Tos P, Perroteau I, Battiston B, Geuna S, Raimondo S, Gambarotta G (2018) Chitosan tubes enriched with fresh skeletal muscle fibers for primary nerve repair. Biomed Res Int 2018:9175248.

Sowa Y, Kishida T, Imura T, Numajiri T, Nishino K, Tabata Y, Mazda O (2016) Adipose-derived stem cells promote peripheral nerve regeneration in vivo without differentiation into schwann-like lineage. Plast Reconstr Surg 137:318e-330e.

Tamaki T, Hirata M, Soeda S, Nakajima N, Saito K, Nakazato K, Okada Y, Hashimoto H, Uchiyama Y, Mochida J (2014) Preferential and comprehensive reconstitution of severely damaged sciatic nerve using murine skeletal muscle-derived multipotent stem cells. PLoS One 9:e91257.

Tamaki T, Okada Y, Uchiyama Y, Tono K, Masuda M, Wada M, Hoshi A, Ishikawa T, Akatsuka A (2007) Clonal multipotency of skeletal muscle-derived stem cells between mesodermal and ectodermal lineage. Stem Cells 25:2283-2290.

Urish KL, Vella JB, Okada M, Deasy BM, Tobita K, Keller BB, Cao B, Piganelli JD, Huard J (2009) Antioxidant levels represent a major determinant in the regenerative capacity of muscle stem cells. Mol Biol Cell 20:509-520.

Vella JB, Thompson SD, Bucsek MJ, Song M, Huard J (2011) Murine and human myogenic cells identified by elevated aldehyde dehydrogenase activity: implications for muscle regeneration and repair. PLoS One 6:e29226.

Walsh S, Biernaskie J, Kemp SW, Midha R (2009) Supplementation of acellular nerve grafts with skin derived precursor cells promotes peripheral nerve regeneration. Neuroscience 164:1097-1107.

Weng J, Wang YH, Li M, Zhang DY, Jiang BG (2018) GSK3β inhibitor promotes myelination and mitigates muscle atrophy after peripheral nerve injury. Neural Regen Res 13:324-330.

Xiang F, Wei D, Yang Y, Chi H, Yang K, Sun Y (2017) Tissue-engineered nerve graft with tetramethylpyrazine for repair of sciatic nerve defects in rats. Neurosci Let 638:114-120.

Yang XN, Jin YQ, Bi H, Wei W, Cheng J, Liu ZY, Shen Z, Qi ZL, Cao Y (2013) Peripheral nerve repair with epimysium conduit. Biomaterials 34:5606-5616.

Zheng M, Duan J, He Z, Wang Z, Mu S, Zeng Z, Qu J, Wang D, Zhang J (2017) Transplantation of bone marrow stromal stem cells overexpressing tropomyosin receptor kinase A for peripheral nerve repair. Cytotherapy 19:916-926.

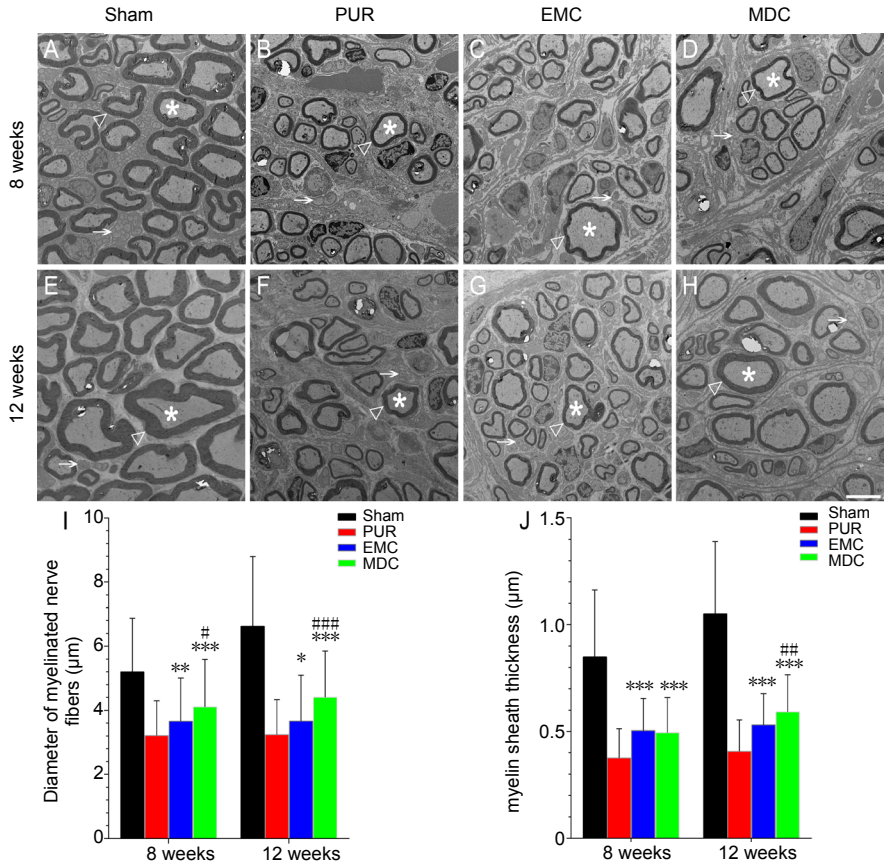

Figure 7 Transmission electron microscopy and morphological evaluation of nerve regeneration at 8 and 12 weeks post-surgery.
(A, E) Sham group; (B, F) PUR group; (C, G) EMC group; (D, H) MDC group. Scale bar: 5 μm. White triangle: myelin sheath; white star: myelinated nerve fibers; white arrow: unmyelinated nerve fibers. Diameter (I) and myelin sheath thickness (J) of myelinated nerve fibers were quantitatively assessed and statistically analyzed. $*P < 0.05$, $**P < 0.01$, $***P < 0.001$, *vs.* PUR group; $\#P < 0.05$, $\#\#P < 0.01$, $\#\#\#P < 0.001$, *vs.* EMC group. Data are expressed as the mean ± SD (number of myelinated nerve fibers from each group: > 100; one-way analysis of variance followed by Bonferroni *post hoc* test). EMC: External oblique muscle-fabricated nerve conduit; MDC: muscle-derived cell; PUR: polyurethane; Sham: sham-operated.

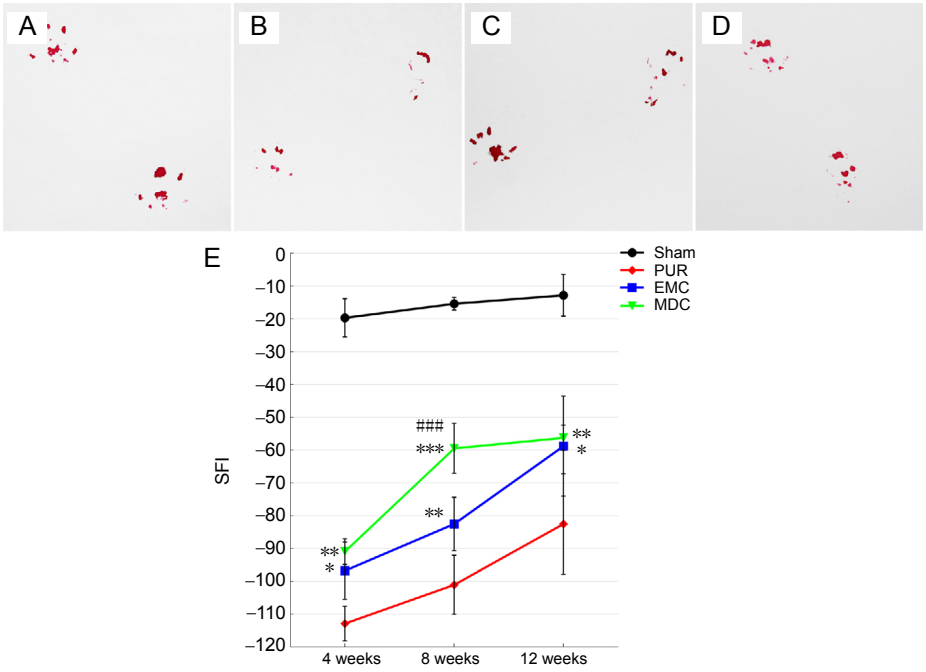

Figure 8 Footprint morphology and SFI at 4, 8, and 12 weeks post-surgery.
(A–D) Typical hind feet tracks at 12 weeks post-surgery in sham, PUR, EMC, and MDC groups, respectively. (E) SFI was quantified to evaluate motor function recovery using hind feet tracks. $*P < 0.05$, $**P < 0.01$, $***P < 0.001$, *vs.* PUR group; $\#\#\#P < 0.001$, *vs.* EMC group. Data are expressed as the mean ± SD (number of footprints from each group: > 5; one-way analysis of variance followed by least significant difference or Bonferroni *post hoc* tests). EMC: External oblique muscle-fabricated nerve conduit; MDC: muscle-derived cell; PUR: polyurethane; SFI: sciatic function index; Sham: sham-operated.

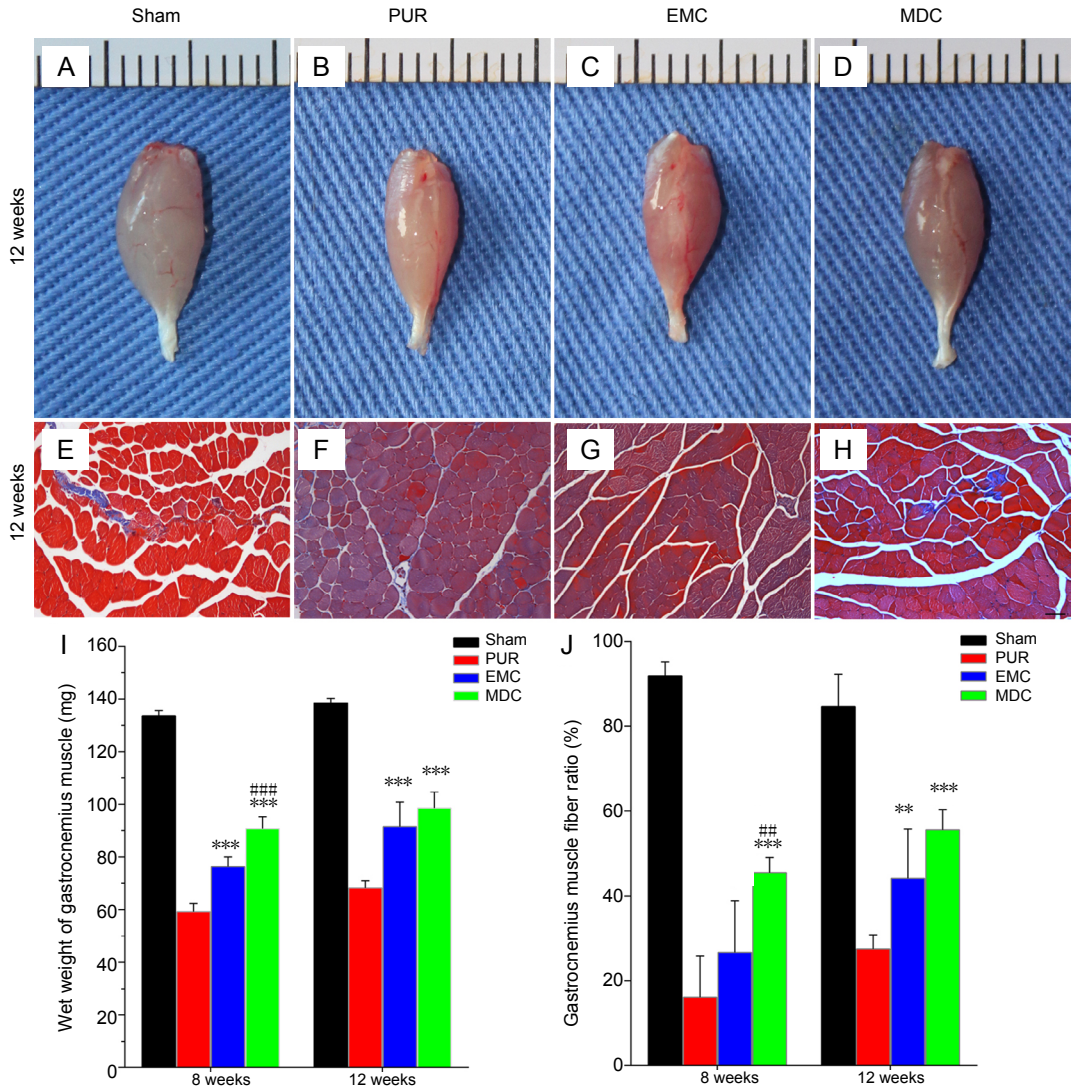

Figure 9 General observation and Masson's trichrome staining of gastrocnemius muscle from the repaired side at 12 weeks post-surgery, and assessment of the wet weight of gastrocnemius muscle and muscle fiber ratio at 8 and 12 weeks post-surgery.
(A–D) General observation and (E–H) cross-sections with Masson's trichrome staining at 12 weeks after surgery. (A, E) Sham group; (B, F) PUR group; (C, G) EMC group; (D, H) MDC group. Scale bar: 100 μm. (I) Wet weight and (J) gastrocnemius muscle fiber ratio were mearsured to evaluate functional recovery of the gastrocnemius muscle. $^{**}P < 0.01$, $^{***}P < 0.001$, *vs.* PUR group; $^{\#\#}P < 0.01$, $^{\#\#\#}P < 0.001$, *vs.* EMC group. Data are expressed as the mean ± SD ($n = 4$; one-way analysis of variance followed by Tukey's *post hoc* test). EMC: External oblique muscle-fabricated nerve conduit; MDC: muscle-derived cell; PUR: polyurethane; Sham: sham-operated.

P-Reviewer: Mert T; C-Editor: Zhao M; S-Editors: Wang J, Li CH;
L-Editors: Qiu Y, Song LP; T-Editor: Jia Y